Journal of Materials Chemistry B

Accepted Manuscript

ROYAL SOCIETY OF CHEMISTRY

www.rsc.org/materialsB

Journal of Materials Chemistry B

PAPER

Improving Antifouling Ability and Hemocompatibility of Poly(vinylidene fluoride) Membranes by Polydopamine-mediated ATRP

Received 00th June 20xx,
Accepted 00th June 20xx

DOI: 10.1039/x0xx00000x

www.rsc.org/

Jinhong Jiang, Peibin Zhang, Liping Zhu*, Baoku Zhu, Youyi Xu

The present work aims to improve the antifouling properties and hemocompatibility of poly(vinylidene fluoride) (PVDF) membranes by polydopamine-mediated atom transfer radical polymerization (ATRP). Polydopamine (PDA) was first prepared by the oxidation and self-polymerization in basic aqueous solution. The obtained PDA was used as an additive in the preparation of PVDF membranes via non-solvent induced phase separation (NIPS). Then poly(sulfobetaine methacrylate) (PSBMA), a commonly used zwitterionic polymer, were successfully grafted from the entrapped PDA in membrane through ATRP. The changes in surface morphologies of the PVDF membranes before and after modification were observed by scanning electronic microscopy (SEM) and atomic force microscopy (AFM). Data of water contact angle measurements indicated that the surface hydrophilicity of the modified membranes was remarkably improved by compared with that of the pure PVDF membrane. Results of filtration tests revealed that the water permeability and antifouling properties of the PVDF membranes were both increased after modification. Moreover, the hemocompatibility of the modified PVDF membrane was greatly improved due to the incorporation of zwitterionic brushes as demonstrated by in vitro platelet adhesion. Owing to the chemical reactivity of polydopamine as well as its strong interactions with a wide spectrum of solid substrates, this strategy can be extended to other materials and allows the development of novel functional membranes through such blending process and secondary treatments.

Introduction

Poly(vinylidene fluoride) (PVDF) is one of the favorable membrane materials because of its excellent mechanical strength, thermal stability, chemical resistance, etc. in contrast to other polymers.[1] Nowadays, commercialized PVDF membranes have been popularized in microfiltration (MF) and ultrafiltration (UF) water treatment, and are promising candidates for biomedical applications such as protein filtration, hemodialysis and hemapheresis.[2-4] However, the inherent hydrophobic nature of PVDF usually gives rise to membrane fouling by adsorbing organics and colloids during separation process. Moreover, activation of coagulation sequence, thrombus formation and other complications are also apt to occur when PVDF is used as bioseparation and blood-contacting materials.[5-7] Therefore, modification is necessary for PVDF membranes to overcome such shortcomings and achieve satisfying lifespan and separation performances in practical uses.[8]

Recently, zwitterionic species, such as phosphotidylcholine, phosphobetaine, sulfobetaine, and carboxybetaine, have been demonstrated as effective and stable modifiers for improving hydrophilicity, non-specific protein resistance and blood compatibility of hydrophobic solid materials.[9-12] An important characteristic of these zwitterions is that they are uniformly mixed with balanced charge, which makes the zwitterionic groups strongly hydrated through ionic solvation.[13] In the reported researches, hydrophobic PVDF membranes have been successfully modified with zwitterionic polymers *via* physisorption, surface grafting, blending, etc.[14-19] The strong electrostatic interactions between water molecules and incorporated zwitterions give rise to the formation of hydration layers at membranes surfaces, thus endowing polymer membranes with good antifouling capacity and hemocompatibility.[20,21] Moreover, the density and chain length of zwitterionic polymers at membranes surfaces also have an important effect on the antifouling properties of the membranes.[12-14] In order to obtain well-defined zwitterionic brushes, surface-initiated atom transfer radical polymerization (ATRP) has been widely developed in surface zwitterionization techniques due to its controlled/living feature and high grafting efficiency.[22-27]

As one of the catecholamines, dopamine as well as its polymers has been found as an useful ATRP initiator precursor that can firmly adhere to a wide range of materials including wood, glass, polymers, ceramic, metal, etc.[28-32] Such catecholamines-initiated ATRP can be applied to nearly any substrates without limit to their surface chemical characteristics, shapes and sizes, which offers novel, effective

MOE Key Laboratory of Macromolecular Synthesis and Functionalization, Department of Polymer Science and Engineering, Zhejiang University, Hangzhou 310027, P.R. China. Email: lpzhu@zju.edu.cn; Tel & Fax: +86 571 87953011

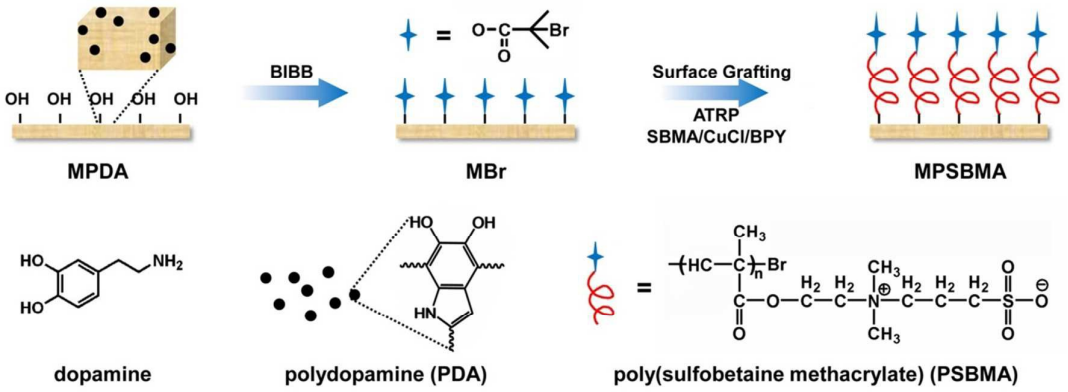

Fig. 1 Scheme for surface grafting of zwitterionic PSBMA onto a PVDF/PDA blend membrane (MPDA) on the basis of PDA-initiated atom transfer radical polymerization (ATRP). (BIBB is the abbreviation of 2-bromoisoburyryl bromide, and BPY is the abbreviation of 2,2′-dipyridyl.)

and versatile strategies to functionalize diverse materials.[33-41] In our previous work, polydopamine (PDA) were synthesized and used as additives to prepare PVDF/PDA blend membranes by non-solvent induced phase separation (NIPS).[42] The incorporated PDA acted as both pore-forming agent and hydrophilic modifier, and opened up opportunities to create multifunctional layers onto the resultant blend membranes through secondary reactions. Thus in this work, antifouling zwitterionic brushes were introduced onto the PVDF/PDA membranes *via* PDA-initiated ATRP to further improve membrane performances for their potential applications in water treatment, bioseparation and blood purification. Compared to PDA coatings reported in previous literatures, blending modification with PDA in this work was helpful to increase retention rate and long-term stability of PDA in membranes. Moreover, the incorporated PDA could not only improve the hydrophilicity and fouling resistance of the membranes, but also act as anchors for antifouling polymer brushes grafted on membrane surfaces via secondary treatments. As shown in Fig. 1, PVDF/PDA blend membranes (MPDA) were first prepared through NIPS process, then brush-like poly(sulfobetaine methacrylate) (PSBMA) were grafted from the surfaces of the MPDA membranes *via* surface-initiated ATRP to produce MPDA-*g*-PSBMA membranes (MPSBMA). The surface morphologies, hydrophilicity, permeability, antifouling properties and hemocompatibility of the modified PVDF membranes were investigated in detail. It is expected that a versatile approach of hydrophilic and biocompatible modification for hydrophobic polymer membranes is established.

Experimental

Materials and Reagents

PVDF resin (solef 1015, M_n = 238 000 g/mol, M_w = 573 000 g/mol) was supplied by Solvey Co., Ltd. Dopamine hydrochloride (dopamine) was purchased from Sigma-Aldrich and used as received. 2-Bromoisoburyryl bromide (BIBB) and 1,3-propanesultone were obtained from Aladdin Reagent Co. and used as received. 2-(Dimethylamino)ethyl methacrylate (DMAEMA, Aladdin) was dried with CaH_2 and distilled under reduced pressure. Triethylamine (TEA), 2,2′-dipyridyl (BPY), bovine serum albumin (BSA), tetrahydrofuran (THF), methanol and acetone were obtained from Sinopharm Chemical Reagent Co., Ltd. TEA was purified by distillation and was stored in 4Å molecular sieves. THF was dried by sodium before use. Copper(I) chloride (CuCl, Sigma-Aldrich) was purified by stirring in acetic acid and washing with ethanol as well as diethyl ether prior to being stored in nitrogen. Platelet-rich plasma (PRP) was supplied by the Blood Center of Zhejiang Province, China. Other chemicals were of analytical grade and used without further purification.

Sulfobetaine methacrylate (SBMA) was synthesized through the reaction of DMAEMA and 1,3-propanesultone following a reported procedure.[43] 1,3-Propanesultone (29.3 g, 240 mmol) dissolved in 50 mL of anhydrous acetone was added dropwise into a solution of DMAEMA (31.4 g, 200 mmol) in 100 mL of dried acetone. After stirring at 0 ºC for about 2 days, the reaction mixture was treated with filtration. The white precipitate was washed with anhydrous acetone and anhydrous ether thoroughly, and then was dried under reduced pressure at room temperature to obtain the final SBMA monomer. The synthesized SBMA monomer was stored at 4 ºC before polymerization. NMR of synthesized SBMA was recorded on a Bruker DPX 400 spectrometer by using D_2O as solvent. ^{1}H NMR (300MHz): δ 6.06(s, 1H, =CH), 5.68(s, 1H, =CH), 4.55 (t, 2H, OCH_2), 3.70 (t, 2H, CH_2N), 3.59 (t, 2H, NCH_2), 3.10 (s, 6H, NCH_3), 2.64 (t, 2H, CH_2COO), 1.84 (s, 3H, $=CCH_3$).

Preparation of Blend Membrane

An aqueous solution of dopamine was prepared by dissolving dopamine (2.0 g, 10.5 mmol) in 2.0 L of deionized water in an open vessel, contacting atmospheric oxygen continuously. Under vigorous stirring, 8 mL of 1 M NaOH solution was added to the solution. After aging for 24 h at 15 ºC, the solution was neutralized with 0.1 M HCl solution and centrifuged at 5000 rpm for 5 min. The polymerization product in the supernatant (PDAP) and polydopamine at the bottom (PDA) were collected under reduced pressure. The powdered PDAP and PDA were

used for characterization and preparation of PVDF/PDA blend membranes.

Pure PVDF membranes (M0) and PVDF/PDA blend membranes (MPDA) were prepared by traditional non-solvent induced phase separation (NIPS) method. PVDF solutions with different additives in N,N'-dimethylacetamide (DMAc) were mixed under stirring at 60 ºC overnight. After degassed under reduced pressure, the solution was casted onto a clean glass plate by using a casting knife with slit width of 250 μm. Then the glass plate was transferred into a coagulation bath of pure water at 40 ºC. The resultant membranes were rinsed in deionized water to remove the residual solvent and unpolymerized dopamine thoroughly. Compositions of each casting solution are listed in Table 1. As reported in our previous study,[42] here PDAP acted as both pore-forming agent and hydrophilic modifier in the NIPS process.

Surface-initiated ATRP of SBMA

MPDA membranes were put into a flask containing 50 mL of THF. Next, 1.6 mL of TEA was added. The flask was put into an ice bath after purged with N_2 for 30 min. Then 1.44 mL of BIBB was added dropwise into the solution with a injector under magnetic stirring. The reaction was performed in N_2 atmosphere for 24 h. The membranes were taken out and washed in acetone, ethanol and deionized water thoroughly. The resultant membrane was referred to as MBr.

PSBMA-grafted membranes were prepared *via* surface-initiated ATRP. First, MBr membranes were put into a three-necked flask filled with 100 mL of 50 % methanol solution ($V_{methanol}$: V_{water} = 1:1). Then SBMA (2.0 g, 7.15 mmol) and BPY (0.31 g, 2 mmol) were added under magnetic stirring. After the system was purged with N_2 for 1 h, CuCl (0.10 g, 1 mmol) was added into the solution. The reaction was conducted under N_2 flow at room temperature for a predesigned time (t). After that the membranes were taken out and washed in ethanol, PBS buffer solution and deionized water thoroughly. The resultant membrane was referred to as MPSBMA.

The graft yield (GY, mg/cm^2) were determined by measuring the weight changes of membranes before and after surface grafting. It was calculated according to Eq. (1):

$$GY = \frac{W_A - W_B}{A} \quad (1)$$

where W_B and W_A (mg) are the weight of the membrane before and after ATRP, respectively. A (cm^2) represents the surface area of the membrane. Each result is an average of three experiments.

Table 1 Compositions of casting solutions for pure PVDF membranes (M0) and PVDF/PDA blend membranes (MPDA).

Membrane ID	PVDF (g)	PDAP (g)	Solvent (mL)	
			Ethanol	DMAc
M0	7.20	0.00	6.00	48.00
MPDA	5.76	1.44	6.00	48.00

Membrane Surface Characterization

Chemical compositions in near surface of pure and modified PVDF membranes were analyzed by X-ray photoelectron spectroscopy (XPS, PHI 5000C ESCA System) with Mg Kα excitation radiation (hν = 1253.6 eV). The binding energies were calibrated by using the containment carbon (C 1s = 284.7 eV). Surface morphologies of the membranes were observed by a field emitting scanning electronic microscopy (FESEM, Hitachi S-4800, Japan). Surface topographies of the membranes were analyzed by an atomic force microscopy (AFM, SPI-3800N, Japan) in tapping mode. The surface roughness was evaluated by root mean square (RMS) based on 1.0 μm × 1.0 μm scan area, and an average of five measurements was reported as the RMS value for each membrane. Surface hydrophilicity of the membranes was characterized by water contact angle measurement (CA, Dataphysics OCA20, Germany) at 20 ºC and 70 % of relative humidity.

Filtration and Antifouling Performance Assessment

A homemade dead-end filtration apparatus with testing area of 4.9 cm^2 was used to measure the permeate flux of the membranes. The filtration test was performed following a reported procedure.[14] A 1.0 g/L protein solution was prepared in advance by dissolving BSA in PBS buffer solution (pH 7.2~7.4). The pure water flux (J_W, L/m^{2}h) and protein solution flux (J_P, L/m^{2}h) of each membrane were recorded and calculated according to Eq. (2) and Eq. (3):

$$J_W = \frac{V_W}{A\Delta t} \quad (2)$$

$$J_P = \frac{V_P}{A\Delta t} \quad (3)$$

where V_W (L) and V_P (L) are the volume of the permeated pure water and protein solution, respectively, A (cm^2) is the effective filtration area (here A = 4.9 cm^2), Δt (h) is the recorded time.

The filtration experiments were operated at a constant pressure of 0.1 MPa. After filtration with pure water for 1 h, the J_W of the membrane was measured and recorded as J_{W1}. Next, the feed solution was replaced with the protein solution, and the J_P was measured after the filtration was performed for 10 h. The membrane was taken out and washed with PBS buffer solution (pH 7.2~7.4) thoroughly, then was shaken in deionized water overnight to remove the reversibly adsorbed proteins. The washed membrane was used for pure water permeation again. After filtration for 1 h, the J_W of the membrane was measured and recorded as J_{W2}. The J_{W1} of the M0 membrane was set as J_0 (J_0 = 5.87 L/m^{2}h), then J/J_0, i.e. J_{W1}/J_0, J_P/J_0 and J_{W2}/J_0, was used to evaluate the permeation properties of each membrane.

The protein rejection (R) was calculated by Eq. (4):

$$R(\%) = (1 - \frac{C_p}{C_f}) \times 100 \quad (4)$$

where C_p and C_f are the protein concentration in the permeate and feed, respectively. The protein concentration was analyzed with a spectrophotometer (Shimadzu, UV-1601) at 280 nm.

The degree of water flux recovery (FR_W) was defined as Eq. (5):

$$FR_W(\%) = (\frac{J_{W2}}{J_{W1}}) \times 100 \quad (5)$$

The degree of flux loss resulting from total protein fouling (R_t) was defined to evaluate the antifouling properties of the membranes. It was calculated using Eq. (6):

$$R_t(\%) = (\frac{J_{W1} - J_P}{J_{W1}}) \times 100 \quad (6)$$

The flux loss caused by both reversible and irreversible protein fouling (R_r and R_{ir}) were calculated according to Eq. (7) and Eq. (8):

$$R_r(\%) = (\frac{J_{W2} - J_P}{J_{W1}}) \times 100 \quad (7)$$

$$R_{ir}(\%) = (\frac{J_{W1} - J_{W2}}{J_{W1}}) \times 100 = 100\% - FR_W \quad (8)$$

Platelet Adhesion

Platelet-rich plasma (PRP, 40 μL) was dropped on membranes that were placed in a 24-well cell culture plate. After incubated statically at 37 ºC for 30 min, each sample was carefully rinsed with PBS buffer solution (PH 7.2) so as to remove non-firmly adherent platelets. Then a 1 wt.% glutaraldehyde solution was prepared and used to fix the platelets on the membrane surface for 30 min. The platelets adhered on the samples were dehydrated with 10, 30, 50, 70, 90 and 100 % (v/v) ethanol/water solution for 20 min in sequence. The resultant samples were kept in a dryer after natural drying and observed with a field-emitting scanning electron microscopy (FESEM, Hitachi S-4800, Japan). The numbers of the adherent platelets on the membranes were calculated according to twenty random representative regions from five SEM images.

Results and Discussion

Polymerization Products in Dopamine Solution

Dopamine and its polymerization products were used as hydrophilic additives in blending modification of PVDF membranes in this work. After centrifuging the dopamine solution that was aged for 24 h, the polymerization product in the supernatant (PDAP) and polydopamine at the bottom (PDA) were characterized with Fourier transform infrared spectra (FT-IR, VECTOR 22, Germany), transmission electron microscopy (TEM, JEM-1230EX, Japan) and Particle Size Analyzer 90 Plus (Brookhaver instruments corporation). Seen from the FTIR spectra presented in Fig. 2A, it was found that PDAP contained both polydopamine (PDA) and unreacted dopamine. Since PDA had similar structures to that of the natural eumelanin,[44] white dopamine turned into dark brown PDAP as the result of polymerization (Fig. 2B). Spherical PDA particles in nano scale were observed in the TEM image of PDAP (Fig. 2C). Their sizes mainly ranged from 45 nm to 114 nm, as shown in Fig. 2D.

During membrane formation process, the unreacted dopamine in the PDAP were released from the nascent film, and the PDA nanoparticles were trapped physically at the surface and in the solidified membranes. Compared with traditional used inorganic nanoparticles, PDA nanoparticles are capable of interacting hydrophobically with PVDF matrix through aromatic rings,[45] which makes them more stable in the as-prepared blend membranes.

Surface Morphology and Wettability

Polydopamine and zwitterionic polymers have been proved to be effective hydrophilic modifiers for hydrophobic polymer membranes.[20,46] Seen from Fig. 3A, the pure PVDF membrane (M0) showed a water contact angle of 96.8º. After blending modification with PDA, the hydrophilicity of the resultant MPDA membrane was notably raised, and the water contact

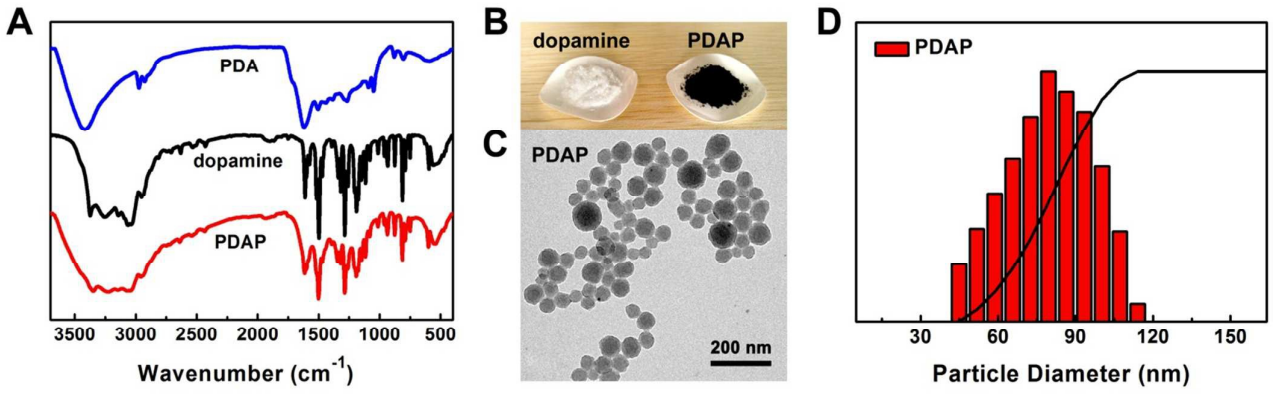

Fig. 2 (A) FTIR spectra of dopamine and its polymerization product. (B) Digital photograph, (C) TEM image and (D) histograms for polymerization product in the supernatant (PDAP).

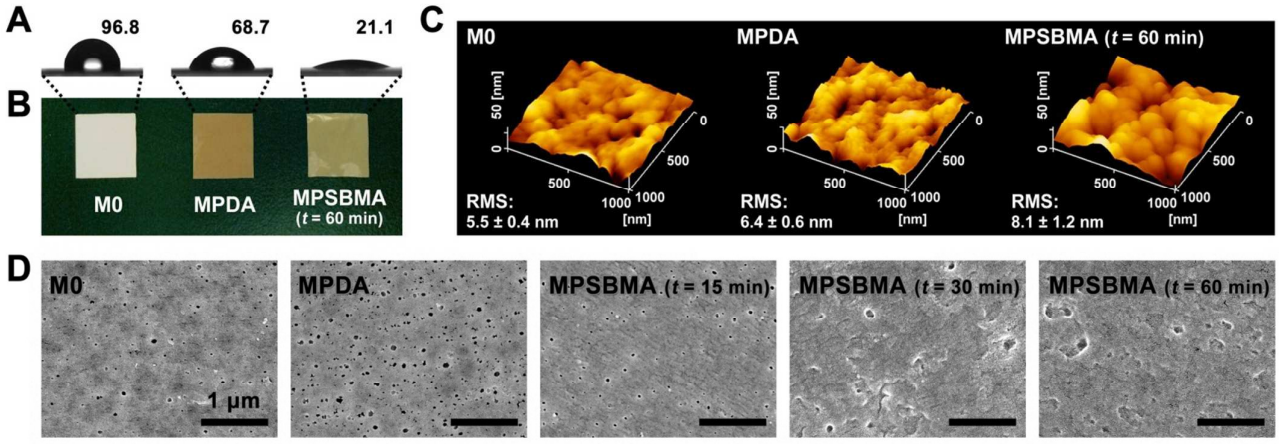

Fig. 3 (A) Water contact angle images, (B) digital photograph, (C) surface AFM topography and (D) SEM images of pure PVDF membrane (M0), PVDF/PDA blend membrane (MPDA) and PSBMA-grafted membranes (MPSBMA) with ATRP time of 15, 30 and 60 min, respectively.

angle reduced to 68.7º correspondingly. The water contact angle of the MPSBMA membrane was further decreased to 21.1º, since strong hydrogen bonding and electrostatic interactions could be formed between PSBMA and water molecules. The water droplet spread quickly along the surface, suggesting the wettability of the membrane was improved significantly. As the result of blending modification, the color of the PVDF membrane turned from white to brown (Fig. 3B), and the surface roughness was increased slightly at the same time (Fig. 3C). The surface grafted-PSBMA layer added luster to the modified membrane somewhat, and the surface roughness of the membrane was further increased because of the incorporation of the PSBMA layer.

The surface SEM images of the membranes are presented in Fig. 3D. Compared with that of the M0 membrane, the surface pores of the MPDA were increased remarkably, which was ascribed to the pore-forming ability of PDAP additives. On one hand, unreacted dopamine and its oligomers were released from the nascent film during NIPS process, leaving pores in the as-prepared solid membranes. On the other hand, the thermodynamic immiscibility was intensified by adding the hydrophilic PDAP additives, which facilitated phase separation and formation of pores. However, owing to the coverage of the PSBMA layer, the surface pores of the MPSBMA membranes were gradually reduced as the ATRP time went on.

Membrane Surface Chemistry

The XPS wide scans of the membranes are shown in Fig. 4, and the surface chemical compositions (at. %) of M0, MPDA,

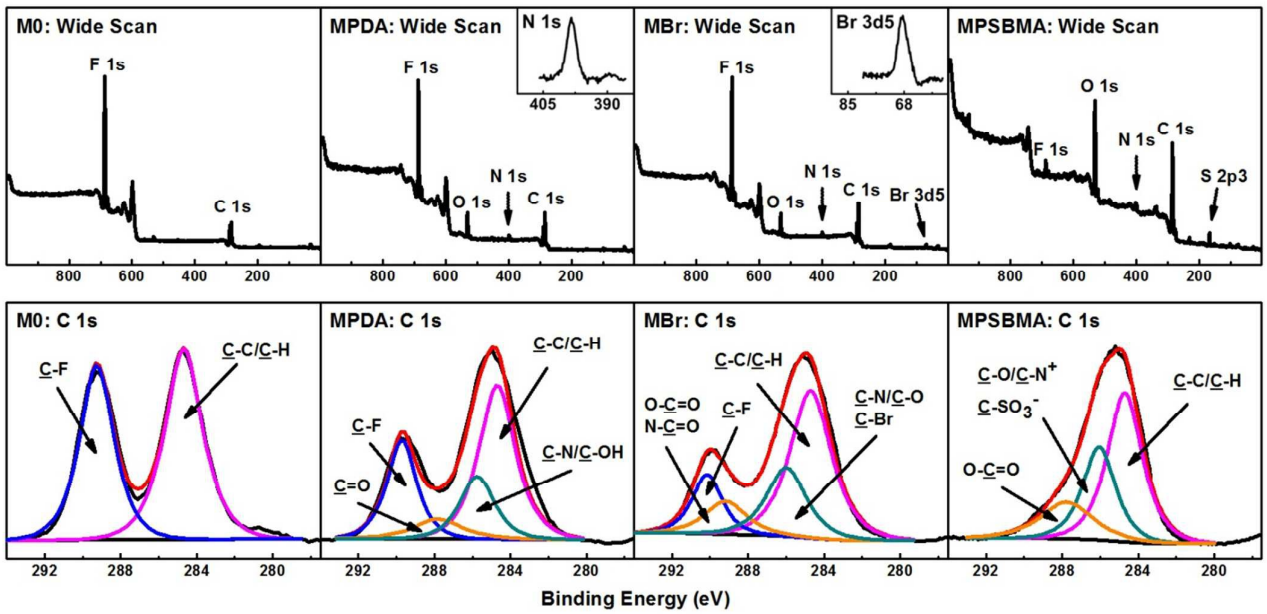

Fig. 4 Typical XPS wide scans and XPS C 1s core-level spectra of the membranes.

MBr and MPSBMA membrane with ATRP time of 2 h are listed in Table 2. Compared with that of the M0 membrane, two new peaks, O 1s (10.3 %, ~532 eV) and N 1s (3.2 %, ~400 eV), were observed in the XPS spectrum of the MPDA membrane. They were assigned to oxygen and nitrogen from polydopamine components in the near surface of the membrane. After the immobilization of BIBB, a new peak Br 3d5 (0.7 %, ~69 eV) appeared in the spectrum of the MBr membrane, indicating the successful incorporation of Br-containing functional groups. For the spectrum of the MPSBMA membrane, the intensities of the O 1s (24.7 %, ~532 eV) and C 1s (65.4 %, ~285 eV) peaks were both increased. Besides, a new peak S 2p3 (3.8 %, ~165 eV) was detected during the measurement, which was due to the sulfur from the grafted PSBMA. It was also found that the peak F 1s (1.8 %, ~687 eV) was still visible in the spectra of the MPSBMA membrane even after zwitterionization. This was probably ascribed to the loss of bound water and subsequent shrinking and cracking of the PSBMA layer during drying process.

Seen from the XPS C 1s core-level spectra, the C 1s of the M0 membrane only had two kinds of peaks, C-F (~289.3 eV) and C-C/C-H (~284.7 eV), while that of the MPDA membrane could be resolved into C=O (~287.8 eV) and C-N/C-OH (~285.8 eV) species additionally. The intensity of the C-F peak obviously reduced, and continued decreasing after esterification. Owing to the immobilization of BIBB, a new peak C-Br occurred in the C 1s core-level spectrum of the MBr membrane. Moreover, it was notable that the C-F peak almost disappeared in the spectrum of the MPSBMA membrane, but a new peak C-O/C-N^+/C-SO_3^- was found at binding energy of ~286.1 eV instead. The results suggested that the zwitterionic polymer had been grafted onto the surface of the PVDF membrane with success.

The effects of ATRP time and SBMA concentration on the graft yield (*GY*) are presented in Fig. 5. It was noted that the variation of *GY* with polymerization time was nearly linear within the initial 120 min. That meant the chain growth from the membrane was broadly in accord with a controlled/living process. Meanwhile, a higher *GY* was obtained when the SBMA concentration was raised from 2 to 4 wt.%. Thus it was implied that *GY* could be adjusted by varying polymerization time or monomer concentration in the surface grafting procedure.

Table 2 Surface chemical composition (at. %) of each membrane calculated from XPS spectra.

Membrane ID	XPS atomic percent (at. %)					
	C	F	O	N	S	Br
M0	51.5	46.2	1.9	0.4	--	--
MPDA	56.4	30.1	10.3	3.2	--	--
MBr	57.3	22.0	17.1	2.9	--	0.7
MPSBMA	65.4	1.8	24.7	4.1	3.8	0.1

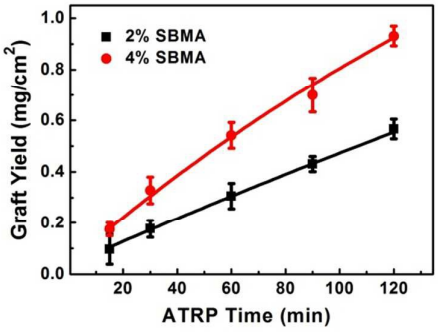

Fig. 5 Dependence of graft yield (GY) on ATRP time and SBMA concentration.

Permeability and Antifouling Property

It is widely known that the non-specific adsorption of organic contaminants especially proteins is the main reason for membrane fouling during separation. In this case, membrane fouling ought to be minimized as much as possible for using membranes efficiently in practical applications. Since BSA is one of the most commonly used model proteins in the investigation of fouling dynamics,[14] it was employed to evaluate the antifouling properties of the membranes in this study. Fig. 6A shows the permeate flux of the PVDF membranes before and after modification. Both of the pure water and protein solution fluxes of the MPDA membrane were more than four times that of the M0 membrane. The addition of PDA raised the porosity and hydrophilicity of the PVDF membrane. This was helpful to reduce the filtration resistance and make water easier to pass through the membrane. As a result, the permeability of the membrane was improved remarkably after blending modification. However, the permeate fluxes of the MPSBMA membranes were decreased in contrast to that of the MPDA membrane, though the hydrophilicity was further increased by surface grafting. The results suggested that the filtration resistance was raised due to the coverage of the PSBMA layer. From Fig. 5 it was known that the graft yield was increased with the ATRP time, thus the permeate fluxes of the MPSBMA membranes were gradually reduced as polymerization time was prolonged.

The BSA rejection (*R*) of each membrane is presented in Fig. 6B. The *R* of the MPDA membrane was lower than that of the M0 membrane, which was probably ascribed to the increases in porosity and pore sizes of the membrane after blending modification. Because the coverage of the PSBMA layer reduced surface pores and pore sizes, the *R* of the MPSBMA membrane was increased with the polymerization time. Furthermore, both of the permeate fluxes and *R* of the MPSBMA membranes with ATRP time less than 30 min were higher than that of the pure PVDF membrane. It was indicated that the separation efficiency of PVDF membranes could be improved under proper modification conditions.

To evaluate the antifouling performances of the membranes, the degree of water flux recovery (FR_W), the degree of flux loss resulting from total protein fouling (R_t), the flux loss caused by

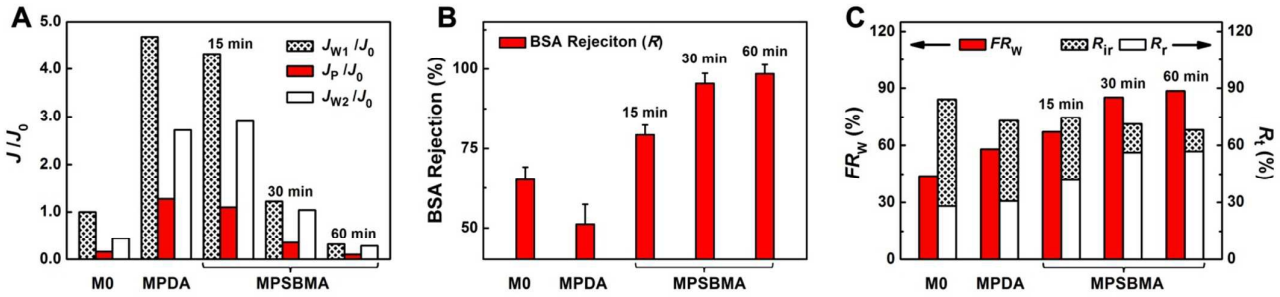

Fig. 6 (A) Permeate flux of water and protein solution through each membrane. (B) Protein rejection and (C) antifouling performances of M0, MPDA and MPSBMA membrane with ATRP time of 15, 30 and 60 min, respectively.

both reversible and irreversible protein fouling (R_r and R_{ir}) were calculated according to Eq. (5-8), where R_r and R_{ir} added together are equal to R_t. Seen from Fig. 6C, the FR_W of the MPDA and MPSBMA membrane were increased by compared with that of the M0 membrane, and the R_t were just the opposite. It was suggested that membrane fouling was reduced due to the hydrophilic modification. Besides, the proportion of R_{ir} in R_t was decreased after blending modification or surface grafting, which meant the irreversible fouling caused by strong adsorption of protein and pore blockage were diminished. Since the reversible fouling could be eliminated by cleaning, the modified membranes exhibited higher degree of water flux recovery than did the M0 membrane. For the MPSBMA membranes, the membrane fouling was decreased with the ATRP time. The grafted-PSBMA are able to bond plenty of water molecules from aqueous solutions *via* strong hydrogen bonding and electrostatic interactions. A hydration layer is formed consequently, hindering the contact of organic contaminants with the membrane surface. In fact, the mobility of the PSBMA chains is also an important factor in antifouling performances. As contaminants move towards the membrane, the repulsion resulting from the steric hindrance suppresses the adsorption of the contaminants on the membrane surface. Moreover, the overall charge neutrality of the zwitterionic PSBMA could usually reduce fouling partly caused by electrostatic adsorption. Thus the antifouling properties of the PVDF membranes were improved significantly after surface grafting.

Hemocompatibility

Platelet adhesion is widely used to evaluate hemocompatibility of various materials since platelet is one of the key factors triggering blood coagulation. Seen from Fig. 7, the numbers and forms of the platelets on unmodified and modified membranes were quite different. Large quantities of platelets (~6.20 × 10^6 cell/cm^2) were found in the SEM image of the M0 membrane. The platelets were in a high degree of deformation and aggregation, for most of them were outspread and aggregate to form clusters. Their irregular shapes and pseudopodium morphologies implied that the activation and transmutation of the platelets were easy to be induced by the pure PVDF membrane. For the MPDA membrane, the number of the adherent platelets (~1.19 × 10^6 cell/cm^2) decreased obviously, though some deformed platelets were still observed

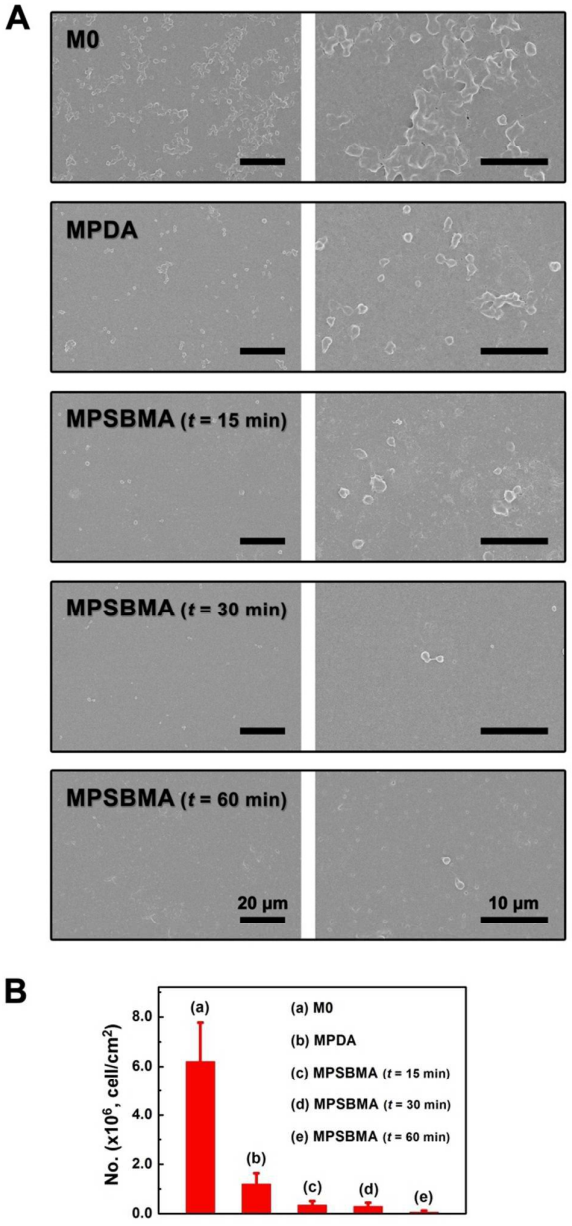

Fig. 7 (A) Morphologies and (B) numbers of platelets adhering on the surfaces of M0, MPDA and MPSBMA membranes with ATRP time of 15, 30 and 60 min, respectively.

on the membrane. After surface grafting of zwitterionic PSBMA, the number of the platelets (ranging from ~0.34 × 10^6 to 0.06 × 10^6 cell/cm^2) decreased further. Only spare platelets were visible on the surfaces of the modified membranes, especially for the MPSBMA membranes with ATRP time of 30 and 60 min. Besides, the adherent platelets exhibited spherical morphologies and kept apart from each other. It was indicated that the adhesion, aggregation and activation of the platelets were suppressed dramatically by the grafted PSBMA layer. Actually, the hydration layer formed on the MPSBMA membrane could act as a natural barrier resisting the non-specific adsorption of proteins such as fibrinogen, thus inhibiting the adhesion and transmutation of platelets in the plasma.[12,21] The results suggested that the hemocompatibility of the PVDF membrane was greatly improved as the result of surface grafting.

Conclusions

Here we demonstrate that the antifouling properties and hemocompatibility of the PVDF membranes could be greatly improved by blending modification and subsequent surface-initiated ATRP. To be specific, PDA was first synthesized and used to prepare PVDF/PDA blend membranes, then zwitterionic PSBMA were successfully grafted onto the blend membranes *via* PDA-initiated ATRP. It is found that the surface pores are reduced after surface grafting due to the coverage of the PSBMA layer, while the surface roughness is raised slightly. The hydrophilicity of the PVDF membrane is significantly improved after modification, and the permeate flux and protein rejection are also increased by compared with that of the pure PVDF membrane. Besides, the modified PVDF membranes show satisfying antifouling properties and hemocompatibility as membrane fouling and adhesion of platelets are both suppressed effectively by the grafted PSBMA layer. This work offers a novel and versatile means to modify hydrophobic polymers based on the versatility and reactivity of polydopamine, which could be extended to different materials for various promising applications in both industrial and scientific fields.

Acknowledgements

The authors are grateful for the financial supports from the National Natural Science Foundation of China (Grant no. 51273176, 51573159), and the Fundamental Research Funds for the Central Universities (Grant No. 2014QNA4038).

References

1 F. Liu, N. A. Hashim, Y. Liu, M. R. M. Abed and K. Li, *J. Membr. Sci.*, 2011, **375**, 1-27.
2 J. F. Hester, P. Banerjee and A. M. Mayes, *Macromolecules*, 1999, **32**, 1643-1650.
3 G. Laroche, Y. Marois, R. Guidoin, M. W. King, L. Martin, T. How and Y. Douville, *J. Biomed. Mater. Res.*, 1995, **29**, 1525-1536.
4 M.-C. Yang and T.-Y. Liu, *J. Membr. Sci.*, 2003, **226**, 119-130.
5 L.-Y. Yu, Z.-L. Xu, H.-M. Shen and H. Yang, *J. Membr. Sci.*, 2009, **337**, 257-265.
6 Y. Chang, Y.-J. Shih, R.-C. Ruaan, A. Higuchi, W.-Y. Chen and J.-Y. Lai, *J. Membr. Sci.*, 2008, **309**, 165-174.
7 L.-P. Zhu, J.-Z. Yu, Y.-Y. Xu, Z.-Y. Xi and B.-K. Zhu, *Colloids Surf., B*, 2009, **69**, 152-155.
8 G.-d. Kang and Y.-m. Cao, *J. Membr. Sci.*, 2014, **463**, 145-165.
9 S. Chen, J. Zheng, L. Li and S. Jiang, *J. Am. Chem. Soc.*, 2005, **127**, 14473-14478.
10 J. Ladd, Z. Zhang, S. Chen, J. C. Hower and S. Jiang, *Biomacromolecules*, 2008, **9**, 1357-1361.
11 S. Jiang and Z. Cao, *Adv. Mater.*, 2010, **22**, 920-932.
12 Y. Chang, Y.-J. Shih, C.-J. Lai, H.-H. Kung and S. Jiang, *Adv. Funct. Mater.*, 2013, **23**, 1100-1110.
13 W. Yang, S. Chen, G. Cheng, H. Vaisocherová, H. Xue, W. Li, J. Zhang and S. Jiang, *Langmuir*, 2008, **24**, 9211-9214.
14 Y.-C. Chiang, Y. Chang, A. Higuchi, W.-Y. Chen and R.-C. Ruaan, *J. Membr. Sci.*, 2009, **339**, 151-159.
15 Z. Yi, L.-P. Zhu, Y.-Y. Xu, X.-N. Gong and B.-K. Zhu, *J. Membr. Sci.*, 2011, **385-386**, 57-66.
16 Y. Chang, W.-J. Chang, Y.-J. Shih, T.-C. Wei and G.-H. Hsiue, *ACS Appl. Mater. Interfaces*, 2011, **3**, 1228-1237.
17 M.-Z. Li, J.-H. Li, X.-S. Shao, J. Miao, J.-B. Wang, Q.-Q. Zhang and X.-P. Xu, *J. Membr. Sci.*, 2012, **405-406**, 141-148.
18 Q. Li, Q.-Y. Bi, B. Zhou and X.-L. Wang, *Appl. Surf. Sci.*, 2012, **258**, 4707-4717.
19 A. Venault, Y. Chang, H.-S. Yang, P.-Y. Lin, Y.-J. Shih and A. Higuchi, *J. Membr. Sci.*, 2014, **454**, 253-263.
20 Y.-H. Zhao, K.-H. Wee and R. Bai, *J. Membr. Sci.*, 2010, **362**, 326-333.
21 Y.-F. Zhao, P.-B. Zhang, J. Sun, C.-J. Liu, Z. Yi, L.-P. Zhu and Y.-Y. Xu, *J. Colloid Interface Sci.*, 2015, **448**, 380-388.
22 J. Ran, L. Wu, Z. Zhang and T. Xu, *Prog. Polym. Sci.*, 2014, **39**, 124-144.
23 R. Barbey, L. Lavanant, D. Paripovic, N. Schüwer, C. Sugnaux, S. Tugulu and H.-A. Klok, *Chem. Rev.*, 2009, **109**, 5437-5527.
24 W.-W. Yue, H.-J. Li, T. Xiang, H. Qin, S.-D. Sun and C.-S. Zhao, *J. Membr. Sci.*, 2013, **446**, 79-91.
25 P.-S. Liu, Q. Chen, S.-S. Wu, J. Shen and S.-C. Lin, *J. Membr. Sci.*, 2010, **350**, 387-394.
26 T. Xiang, L.-S. Zhang, R. Wang, Y. Xia, B.-H. Su and C.-S. Zhao, *J. Colloid Interface Sci.*, 2014, **432**, 47-56.
27 Y. Zhang, Z. Wang, W. Lin, H. Sun, L. Wu and S. Chen, *J. Membr. Sci.*, 2013, **446**, 164-170.
28 H. Lee, S. M. Dellatore, W. M. Miller and P. B. Messersmith, *Science*, 2007, **318**, 426-430.
29 X. Fan, L. Lin, J. L. Dalsin and P. B. Messersmith, *J. Am. Chem. Soc.*, 2005, **127**, 15843-15847.
30 B. Zhu and S. Edmondson, *Polymer*, 2011, **52**, 2141-2149.
31 S. M. Kang, N. S. Hwang, J. Yeom, S. Y. Park, P. B. Messersmith, I. S. Choi, R. Langer, D. G. Anderson and H. Lee, *Adv. Funct. Mater.*, 2012, **22**, 2949-2955.
32 J. Kuang and P. B. Messersmith, *Langmuir*, 2012, **28**, 7258-7266.
33 H. Hu, B. Yu, Q. Ye, Y. Gu and F. Zhou, *Carbon*, 2010, **48**, 2347-2353.
34 W.-C. Wang, J. Wang, Y. Liao, L. Zhang, B. Cao, G. Song and X. She, *J. Appl. Polym. Sci.*, 2010, **117**, 534-541.
35 C. Y. Li, W. C. Wang, F. J. Xu, L. Q. Zhang and W. T. Yang, *J. Membr. Sci.*, 2011, **367**, 7-13.
36 W. O. Yah, H. Xu, H. Soejima, W. Ma, Y. Lvov and A. Takahara, *J. Am. Chem. Soc.*, 2012, **134**, 12134-12137.
37 Y. Sui, X. Gao, Z. Wang and C. Gao, *J. Membr. Sci.*, 2012, **394-395**, 107-119.
38 C. Rodriguez-Emmenegger, C. M. Preuss, B. Yameen, O. Pop-Georgievski, M. Bachmann, J. O. Mueller, M. Bruns, A. S.

Goldmann, M. Bastmeyer and C. Barner-Kowollik, *Adv. Mater.*, 2013, **25**, 6123-6127.
39 J.-L. Shi, L.-F. Fang, H. Li, H. Zhang, B.-K. Zhu and L.-P. Zhu, *J. Membr. Sci.*, 2013, **437**, 160-168.
40 L.-J. Zhu, F. Liu, X.-M. Yu, A.-L. Gao and L.-X. Xue, *J. Membr. Sci.*, 2015, **475**, 469-479.
41 M.-C. Sin, Y.-M. Sun and Y. Chang, *ACS Appl. Mater. Interfaces*, 2014, **6**, 861-873.
42 J.-H. Jiang, L.-P. Zhu, H.-T. Zhang, B.-K. Zhu and Y.-Y. Xu, *J. Membr. Sci.*, 2014, **457**, 73-81.
43 Z. Zhang, T. Chao, S. Chen and S. Jiang, *Langmuir*, 2006, **22**, 10072-10077.
44 K.-Y. Ju, Y. Lee, S. Lee, S. B. Park and J.-K. Lee, *Biomacromolecules*, 2011, **12**, 625-632.
45 J. Yu, Y. Kan, M. Rapp, E. Danner, W. Wei, S. Das, D. R. Miller, Y. Chen, J. H. Waite and J. N. Israelachvili, *Proc. Natl. Acad. Sci. U.S.A.*, 2013, **110**, 15680-15685.
46 Z.-Y. Xi, Y.-Y. Xu, L.-P. Zhu, Y. Wang and B.-K. Zhu, *J. Membr. Sci.*, 2009, **327**, 244-253.

A versatile strategy for preparation of polymer membranes with remarkably improved antifouling properties and hemocompatibility is developed through simple blending process and secondary treatments.